Available online at www.sciencedirect.com
SCIENCE DIRECT
Journal of Catalysis 236 (2005) 153–163
JOURNAL OF CATALYSIS
www.elsevier.com/locate/jcat

Modeling of kinetics and deactivation in the direct epoxidation of propene over gold–titania catalysts

T. Alexander Nijhuis [a,*], Tracy Q. Gardner [b], Bert M. Weckhuysen [a]

[a] *Department of Inorganic Chemistry and Catalysis, Debye Institute, Utrecht University, Sorbonnelaan 16, 3584 CA Utrecht, The Netherlands*
[b] *Chemical Engineering Department, Colorado School of Mines, 1613 Illinois Street, Golden, CO 80401, USA*

Received 11 August 2005; revised 16 September 2005; accepted 19 September 2005

Abstract

A reaction model was developed for the epoxidation of propene oxide over gold–titania catalysts. This model involves the formation of a bidentate propoxy species on titania after the adsorption of propene, which is activated by gold. Aided by a peroxide species produced from hydrogen and oxygen on a gold nanoparticle, this species can reactively desorb from the catalyst to produce propene oxide. A reversible catalyst deactivation occurs by a consecutive oxidation of the bidentate propoxy species to carbonate species. The kinetic model is able to give a good description of the experimentally observed catalytic performance in the low-temperature range (up to 365 K), where the selectivity of the catalyst is high.

Keywords: Gold; Titania; Propene; Epoxidation; Mechanism; Kinetic modeling

1. Introduction

The epoxidation of propene over gold–titania catalysts has attracted considerable attention over the past years since it was discovered as a selective catalyst system for the direct epoxidation of propene [1]. Both gold and titania seem to be necessary for this type of catalyst to be able to epoxidize propene. The common assumption postulated in the literature is that the reaction mechanism involves a peroxide species produced by gold [2,3]. This peroxide species would thereafter epoxidize propene over titania sites. This assumption for a reaction model is supported by the facts that both oxygen and hydrogen are necessary for this oxidation reaction and that propene can be epoxidized by hydrogen peroxide over titania [4]. Theoretical calculations have indeed shown that OOH [5] or even hydrogen peroxide [6,7] can be formed on small gold particles. This has been confirmed experimentally for both the gas [3] and liquid phases [8]. However, no conclusive evidence exists that this also occurs during the propene epoxidation reaction, making this peroxide mechanism speculative.

Recently we elaborated on the role of gold in the activation of propene, based on the results of an infrared spectroscopic study on Au/TiO_2 catalysts [9]. We showed that gold nanoparticles could induce the formation of an adsorbed bidentate propoxy species on titania. This bidentate species could be oxidized and further catalyzed by the gold nanoparticles to produce strongly adsorbed carbonate/carboxylate species, most likely connected to catalyst deactivation. In the present paper, this knowledge of the surface species is linked to the performance of the catalyst, and a reaction mechanism is proposed. A kinetic model based on this mechanism is fitted to the catalytic experiments, and rate constants and activation energies for the catalytic steps are determined.

2. Experimental

2.1. Catalyst preparation

Gold was deposited on titania (P25, Degussa; 70% anatase, 30% rutile, 45 m^2/g) by a deposition precipitation method [2]. Five grams of titania were dispersed in 100 mL of demineral-

* Corresponding author. Fax: +31 30 2511027.
E-mail address: t.a.nijhuis@chem.uu.nl (T.A. Nijhuis).

0021-9517/$ – see front matter
doi:10.1016/j.jcat.2005.09.027

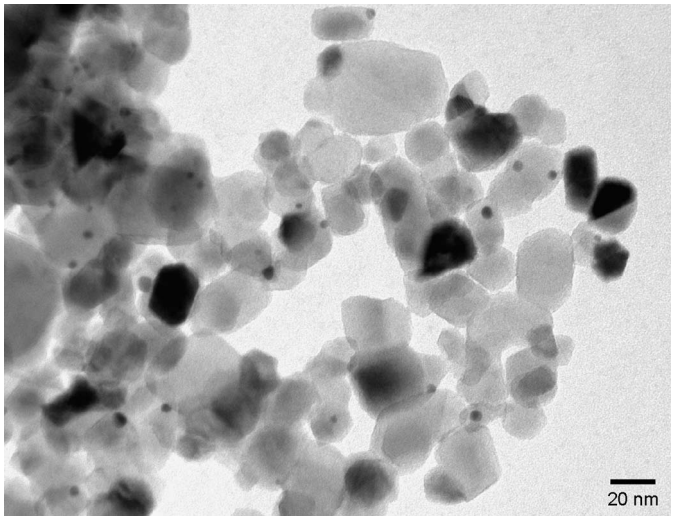

Fig. 1. TEM micrograph of 1 wt% gold on P25 titania catalyst.

ized water with a magnetic stirrer. The pH of the slurry was 3.8. Using 2.5% ammonia,[1] the pH was raised to 9.5. Next, 300 mg of a $HAuCl_4$ solution (17 wt% Au) was dissolved in 20 mL of demineralized water and added slowly (over about 15 min) to the support slurry. While the gold solution was being added, the pH was continuously adjusted to remain between 9.4 and 9.6. After the gold was added, the solution was stirred for 30 min, after which it was filtered and washed 3 times with 200 mL of demineralized water. The yellow catalyst was dried overnight in an oven at 333 K and then calcined. Calcination was carried out by heating to 393 K (at a rate of 5 K/min) for 2 h, followed by 4 h at 673 K (5 K/min heating and cooling). The catalysts obtained had an intense purplish-blue color.

2.2. Catalyst characterization

X-ray fluorescence (XRF) analysis showed that the gold loading on the catalysts was always close to the target loading of 1 wt%. The catalyst typically contained 95% of the amount of gold precursor used. The amount of chloride on the catalysts, a common contaminant affecting the activity, was below the detection limit (<6 μg/g). Transmission electron microscopy (TEM) analysis (Fig. 1) showed an average gold particle size of 4.0 nm, with a standard deviation of 1.1 nm (average of approximately 250 gold particles). Energy-dispersive X-ray analysis using TEM on areas where no gold particles were visible did not reveal any gold. These observations indicate that, within the sensitivity limits of the techniques used, no sub-1-nm "invisible" gold was present on the catalysts. Scanning electron microscopy analysis showed that the 20–50 nm primary titania particles formed aggregates of larger (5–20 μm) particles.

[1] When preparing gold catalysts using a deposition precipitation using ammonia care should be taken that the possibility exists of forming highly explosive fulminating gold. In the preparations in this paper the risks are very minor considering the small quantities of gold and the low loadings on the catalysts prepared. Care is advisable however considering a recently reported incident (explosion) [10]. It is recommended that readers take the advantages (ease of making stable catalysts without chloride or sodium present) and disadvantages of this preparation method into consideration.

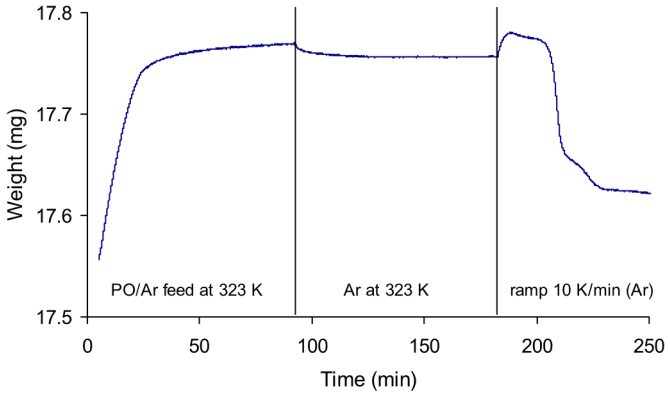

Fig. 2. Example of thermogravimetrical adsorption–desorption experiment: adsorption of propene oxide on P25 titania in argon atmosphere.

Table 1
Summary of thermogravimetrical adsorption experiments. Adsorption of propene oxide gas at 323 K followed by desorption (first isothermal at 323 K, then heating to 773 K, values corrected for mass changes recorded in a blank run, error ±0.02 wt%)

Catalyst support	Gas	Relative weight change after (%)		
		Adsorption (323 K)	Desorption (323 K)	Desorption (773 K)
P25 (titania)	Argon	+1.50	+1.42	+0.36
P25 (titania)	20% O_2 in argon	+1.50	+1.40	−0.14
Au/P25	Argon	+1.42	+1.31	+0.03
Au/P25	20% O_2 in argon	+1.52	+1.41	−0.16

Thermogravimetric experiments were carried out to determine the adsorption capacity of the catalyst for the desired product, propene oxide. In these experiments, propene oxide was adsorbed on the dried catalyst (at 323 K), and physisorbed propene oxide was allowed to desorb at the same temperature, after which the sample was heated at a rate of 10 K/min up to 773 K, to allow desorption or decomposition of the adsorbed species. These experiments were carried out in argon and in a 20% oxygen in argon atmosphere. Fig. 2 shows an example is shown of such an experiment; Table 1 gives the determined adsorption capacities. The presence of gold particles did not measurably change the adsorption capacity of propene oxide. Comparing the experiments in argon and oxygen/argon reveals that the catalyst loses all adsorbed species only when it is heated in the presence of oxygen. The small weight decrease for these measurements is caused by the loss of adsorbed water at the high final temperature. Heating in an argon stream results in a catalyst whose weight has increased at the final temperature of the thermogravimetric experiment. This indicates that the adsorption of propene oxide is not reversible and that decomposition products remain on the catalyst surface. Heating the catalyst in artificial air (oxygen/argon mix) combusts the decomposition products. Comparing the temperature-programmed desorption in artificial air of propene oxide with and without gold shows that during heating, a small weight increase initially occurred when gold was present but did not occur without gold (not shown). This finding agrees with the infrared adsorption

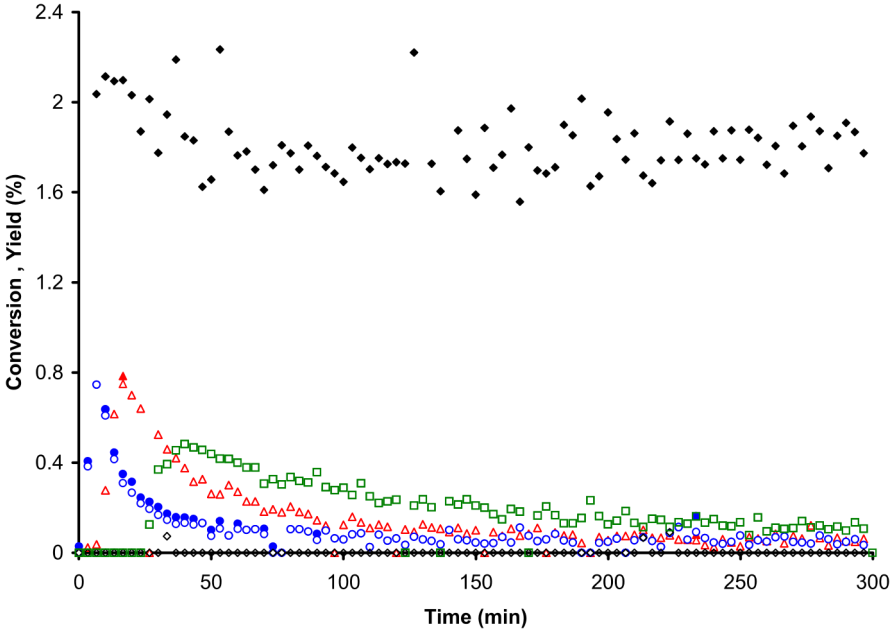

Fig. 3. Catalytic performance of Au/TiO_2 catalyst. Conversion (closed symbols) and yield (open) at 323 (□), 343 (△), 363 (○), and 423 K (●) (pressure 1.1 bar, GHSV 9000 $m^3_{gas}/(m^3_{cat}\,h)$) (yield and conversions largely overlap for experiments at 323 and 343 K).

experiments showing that gold can oxidize adsorbed species. The thermogravimetrically determined adsorption capacity is used as an input for the kinetic model.

2.3. Catalyst activity testing

A flow reactor was used to determine the catalytic performance. The experiments were typically carried out with 0.35 g of catalyst and a gas flow of 50 NmL/min (GHSV = 9000 $m^3_{gas}/(m^3_{catalyst}\,h)$. The catalyst masses used ranged from 0.2 to 0.45 g, and flow rates varied from 25 to 250 NmL/min. The reactor had a 4-mm inner diameter and typically a 3-cm bed height. The gas mixture consisted of 10% oxygen, 10% hydrogen, and 10% propene in helium (all gas compositions given in vol%). The gas leaving the reactor was analyzed using an Interscience Compact gas chromatography system equipped with a Molsieve 5A and a Porabond Q column, each with a thermal conductivity detector. Gas samples were analyzed every 3 min. The temperature of the catalyst bed was measured using to thermocouple in the bed to determine possible heat effects. The experiments were carried out in cycles: 5 h at a reaction temperature with the reactant mixture, followed by a regeneration cycle. During regeneration, 10% oxygen in helium was flowed over the catalyst, which was heated to 573 K (at a rate of 10 K/min) and maintained at this temperature for 1 h. Then the catalyst was cooled to the next reaction temperature in the cycle. The performance was tested at reaction temperatures ranging from 313 to 473 K. Periodically, duplicates were measured to determine the extent of catalyst deactivation.

Fig. 3 shows an example of three reaction cycles conducted at different temperatures, and Fig. 4 summarizes the catalytic performance at different temperatures. In the experiments represented in Figs. 3 and 4, within a 5-h catalytic cycle, the activity for the P25-supported catalyst first increased and then

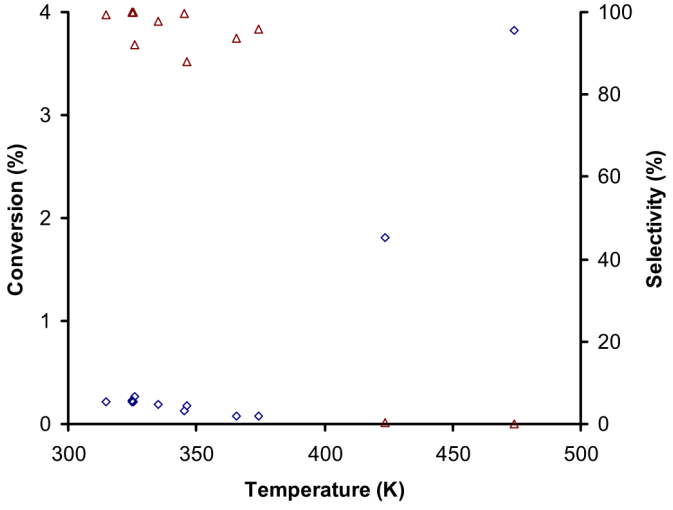

Fig. 4. Catalytic performance as a function of temperature (average values from 30 to 270 min within a catalytic cycle). Conversion (◇), selectivity (△). 1 wt% Au/TiO_2 (P25) catalyst (0.3 g catalyst, gas flow 50 NmL/min, 10% hydrogen, oxygen, and propene in helium).

decreased rapidly (at 30%/h). However, although losses in catalytic activity could be observed within a cycle, the activity could be completely restored in the regeneration procedure at 573 K in oxygen/helium. After regeneration, the catalyst exhibited an identical catalytic activity. Irreversible deactivation was not observed, even after as many as 50 catalytic cycles.

The main side products are water, carbon dioxide, methanol, acetone, propanal, acrolein, and ethanal. At the lower temperatures, the side products are primarily ethanal and carbon dioxide; at higher temperatures, propanal and acrolein are also formed in larger quantities. Propane was not observed as a side product for this catalyst. Very rapid deactivation, as was observed for propene oxide, did not occur for the side products.

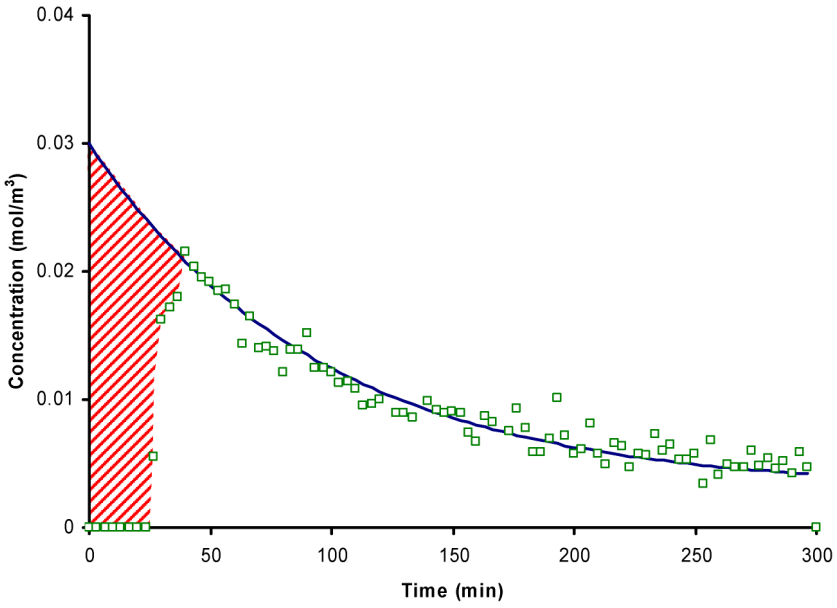

Fig. 5. Catalytic performance of Au/TiO_2 catalyst. Measured conversion at 323 K (□), and extrapolation of the catalytic activity in the absence propene oxide adsorption on the titania (drawn line). The marked area represents the propene oxide 'lost' by adsorption (pressure 1.1 bar, GHSV 9000 $m^3_{gas}/(m^3_{cat}\,h)$).

Examining the catalytic activity plots reveals that it determining a simple rate constant or activation energy for this reaction system is difficult. At the lower temperatures, a dead time occurs before products are observed, followed by a rapid increase in activity, and finally a gradual decline in activity. Simply taking the "steady-state" activity of the catalyst, the propene oxide production rate appears to be higher at lower temperatures, resulting in a negative activation energy, which is uncommon and unlikely because at the beginning of a catalytic cycle, propene oxide production increases with increasing temperature. This observation also rules out the possibility of the heat of adsorption of propene being higher than the activation energy for the epoxidation, causing an apparent negative activation energy. The decreasing steady-state propene oxide production with increasing reaction temperature can be explained if the activation energy for the epoxidation is lower than the activation energy for the catalyst deactivation. Therefore, it is necessary to develop a complete kinetic model, which takes both reaction and deactivation into account, to determine the kinetic parameters.

3. Reaction mechanism

In this discussion on the kinetic mechanism, the primary focus is on the experiments at temperatures $\leqslant$373 K. At higher temperatures, the selectivity of the catalyst drops significantly because of competing side reactions, making kinetic evaluation very complex. For the titania-supported catalyst, the activity goes through a maximum within a catalytic cycle. This behavior can be explained by two processes: (1) adsorption of propene oxide on the catalyst (or support) until the adsorption capacity is reached, and (2) deactivation of the catalyst. These processes are depicted in Fig. 5, with the drawn curve representing the "true" catalytic activity and the marked area indicating the amount of propene oxide remaining on the catalyst. The amount of propene oxide retained in the reactor can be determined by integrating the area under the curve. For the experiment shown in Fig. 5, the propene oxide retained amounts to 0.69 wt%. Comparing this with the propene oxide adsorption capacity as determined thermogravimetrically (1.4 wt%) reveals that the amount retained in Fig. 5 can be easily explained by this adsorption capacity. The fact that the adsorbed amount is about half of the amount measured thermogravimetrically can be explained by considering the competitive adsorption of water [11] during the reaction. This competitive adsorption was also observed experimentally in a study on the effect of water on epoxidation over gold–titania catalysts [12].

Activity extrapolations like those shown in Fig. 5 were made for a series of experiments at different flow rates and temperatures. Fig. 6 shows the initial propene oxide yields (to $t = 0$) determined from these extrapolations. It can be seen that the extrapolated initial reaction rate does indeed increase with temperature. The fact that reaction rate does not exponentially increase with temperature according to the Arrhenius equation also indicates that the initial propene oxide formation kinetics are more complex and most likely consist of different reaction steps in series. From the data points at the lowest temperatures, an apparent activation energy of 30 kJ/mol can be calculated for the propene oxide production. As a function of the space velocity, the initial propene oxide production rate is constant. This is as expected for a reaction at very low conversion levels, and indicates that the reaction is dictated by the primary formation of propene oxide and not much affected by its consecutive reactions. The constant reaction rate as a function of gas hourly space velocity (GHSV) also indicates that mass transfer effects play no role in this system. The amount of adsorbed propene oxide adsorbed that can be calculated from these extrapolations was similar (approximately 0.7 wt%) at all flow rates and temperatures. This indicates that propene oxide is irreversibly adsorbing at these lower temperatures rather than re-

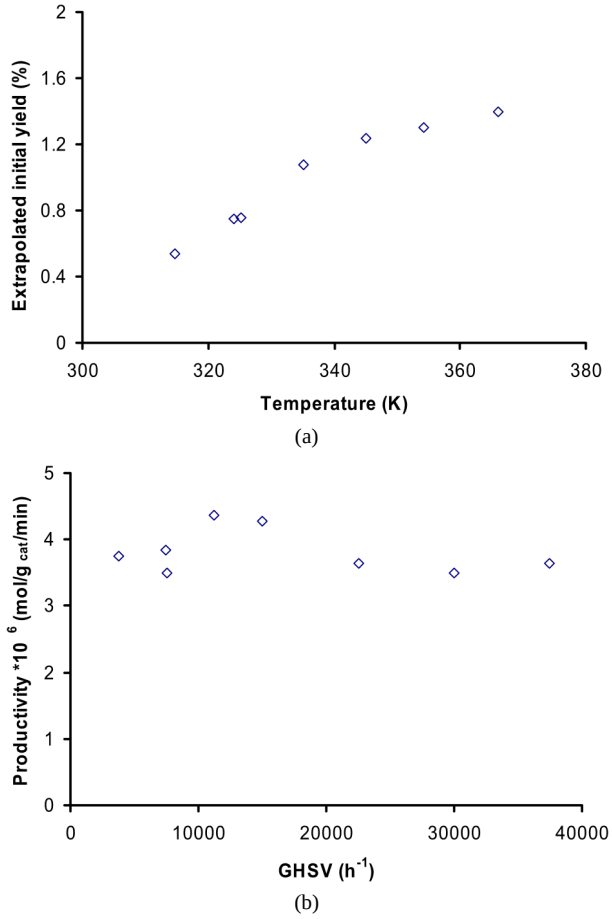

Fig. 6. Initial activity at $t = 0$ in a catalytic cycle, determined by extrapolating the propene oxide yield. (a) Initial activity as a function of temperature (pressure 1.1 bar, GHSV 9000 $m^3_{gas}/(m^3_{cat}\,h)$). (b) Initial activity as a function of GHSV (pressure 1.1 bar, $T = 323$ K).

versibly physically absorbing, which is also in agreement with the thermogravimetric experiments in which we also did not see propene oxide desorbing below 573 K. It should be noted, however, that these estimations made for propene oxide adsorbed at the higher temperatures have a relatively large error, which may be obscuring a trend.

The gold catalysts used in this study all tend to deactivate rapidly. But this rapid deactivation is reversible as far as can be observed on a time scale of up to 15 days. Once the catalyst has been regenerated at 573 K in an air stream, the catalytic activity is completely restored. After up to 50 reaction–regeneration cycles, the selectivity of the catalyst remains unchanged, and the activity is still at least 90% of the activity of the fresh catalyst. This small loss in activity after such a relatively long operation is negligible compared with the rapid deactivation occurring within a catalytic cycle. This rules out the possibility that the rapid deactivation occurs through sintering of the gold particles. Furthermore, TEM micrographs did not show any significant differences in the size of the gold particles between "fresh" and "spent" catalysts. Therefore, the formation or accumulation of an activity-inhibiting species on the catalyst surface provides a better explanation for the rapid deactivation. The first suggestion in the literature was that these were oligomeric species of propene oxide [2,13]; however, later papers studying surface species using infrared spectroscopy failed to find such species on the catalyst surface [9,14]. Recently, we found that gold particles are capable of converting adsorbed propene oxide into carbonate/carboxylate species, which do not easily desorb from the surface and are likely candidates for the deactivating species [9]. Attempts to describe the catalyst deactivation with simple time dependant engineering correlations were not successful; therefore, it is necessary to set up a kinetic model for the reaction system that also includes the formation of the deactivating species in the rate expression. From the fact that after the initial period the propene oxide yield decreases with increasing reaction temperature, even though no side (consecutive) products are observed, it can be concluded that in the kinetic model, the activation energy for deactivation must be higher than the activation energy for propene oxide production.

Consequently, based on our catalytic data and observations and on mechanistic suggestions reported in the literature, we propose a model consisting of the following processes occurring in the reactor:

1. Production of propene oxide from propene reactively adsorbing on catalytic gold/titania sites.
2. Desorption of propene oxide from catalytic sites aided by a peroxide species produced from hydrogen and oxygen.
3. Adsorption of propene oxide on catalytic sites.
4. Adsorption of propene oxide on noncatalytic titania sites.
5. Oxidation of propene oxide adsorbed on catalytic gold/titania sites to carbonates/carboxylates (formation of deactivating species on the catalyst).

The first and most important step in this sequence requires the presence of both gold and titanium (as TiO_2 or Ti dispersed on or in an oxidic support). Titania alone has no activity for the epoxidation of propene with hydrogen and oxygen. Gold on silica does not produce significant quantities of propene oxide either. Some other metals cooperating with titania also have some epoxidation activity, but their performance is considerably worse than that of gold. Only silver shows some promise for this reaction system [15,16].

In step 2, propene oxide desorbs from the catalyst, aided by hydrogen and oxygen. This step is based on observations in our previous studies in an infrared cell demonstrating that feeding hydrogen and oxygen at reaction temperature caused the bidentate propoxy species to desorb [9]. This is also supported by the fact that propene oxide is observed only with both hydrogen and oxygen present. In previous studies [2,3], a peroxide species was commonly assumed to be a key reaction intermediate in propene epoxidation using hydrogen/oxygen over gold–titania catalysts. The expectation that such a species would be a key reaction intermediate results primarily from the good epoxidation activity of titania catalysts when a peroxide is used as an oxidant [4]. But a peroxide species was not observed in our studies using infrared and Raman spectroscopy, even though Raman is quite sensitive toward peroxides. Product desorption is the rate-determining step, according to our observations and earlier reports [2,11]. Therefore, the predominant species on the catalyst

surface should be adsorbed propene oxide, which can be present in the form of the bidentate propoxy that we observed. A peroxide species can still play a key role in the reaction mechanism, considering our observation that hydrogen and oxygen aid in the desorption of the bidentate propoxy species. The assumptions that peroxide formation is necessary to aid in the desorption of the propene oxide/bidentate propoxy, and that the formation of this peroxide species is the rate-determining step, imply that the concentration of the peroxide species would be very low. Consequently, the concentration of this peroxide species may simply be beyond the sensitivity limits of our equipment. The formation of peroxide species (OOH or H_2O_2) on gold from hydrogen and oxygen has been confirmed experimentally [3,17]. Moreover, theoretical calculations have demonstrated that these peroxide species are likely formed [5,6]. These findings support a reaction model in which a peroxide species is formed on the gold particles in the rate-determining step, which reacts with the bidentate propoxy species to produce propene oxide. Such a model is in agreement with our experimental observations.

Consequently, we propose the following reaction mechanism for the formation of propene oxide:

1. Propene reacts with titania to produce an adsorbed bidentate propoxy species. This reaction is catalyzed by the gold nanoparticles present on the titania.
2. Hydrogen and oxygen produce a hydroperoxide species (OOH or H_2O_2) on gold.
3. The peroxide species aids the desorption of the bidentate propoxy species from the catalyst, producing propene oxide and water and restoring the titania to its original state.

A question for the first step of this reaction mechanism is "What is the oxygen source for the bidentate species that we are forming on the catalyst surface?" In the infrared propene adsorption experiments, this species was formed without the presence of gas-phase oxygen. Therefore, in these experiments the oxygen source must have been the titania. It is known that titania can be reduced, or can donate oxygen, under mild conditions [18,19]. In a continuous catalytic experiment, however, the amount of oxygen the titania can donate is limited. Therefore, either the catalytic cycle must be closed by a reoxidation of the surface or this oxidation must also occur with a different oxygen source (i.e., gas-phase oxygen or a peroxide species produced on the gold). In our proposed kinetic model, we choose the option to close the catalytic cycle by simultaneous reoxidation of the titania and propene oxide desorption by a reaction with a peroxide species. For catalyst deactivation [Eq. (2)], we similarly used lattice oxygen as an oxidant in the kinetic model, because in infrared experiments this reaction occurred without feeding oxygen [9,20]. However, in a catalytic experiment this deactivation occurs at a time scale of minutes, whereas in the infrared experiments this reaction occurs at a much slower rate (approximately 20 h for complete oxidation). Therefore, it is likely that the faster oxidation of the bidentate propoxy species in the catalytic experiments is the result of oxidation with oxygen or a peroxide species. Conclusive evidence about the oxygen source for propene epoxidation and catalyst deactivation should come from isotopic experiments.

Table 2
Model representing the key steps in the propene epoxidation over gold-titania catalysts

$$C_3H_6 + 2Ti_{Au} + 2O_{TiO_2} \rightarrow BPS_{Au} \quad (1)$$

$$H_2 + O_2 + Au \rightarrow Au\text{–}HOOH \quad (2)$$

$$Au\text{–}HOOH + BPS_{Au} \rightarrow PO + H_2O + Au + 2Ti_{Au} + 2O_{TiO_2} \quad (3)$$

$$BPS_{Au} + xO_{TiO_2} \rightarrow 2Ti_{Au}\text{–Carbox} \quad (4)$$

$$PO + 2Ti_{Au} + O_{TiO_2} \rightarrow BPS_{Au} \quad (5)$$

$$PO + 2Ti_{Ti} + O_{TiO_2} \rightarrow BPS_{Ti} \quad (6)$$

With

C_3H_6	gas phase propene
BPS	bidentate propoxy species
Ti	Titania site (Ti–O–Ti or Ti–OH)
O	lattice oxygen
PO	gas phase propene oxide
Carbox	carbonate/carboxylate/formiate species
x	value > 0 (oxygen consumed for BPS oxidation)

Subscripts

Au	neighboring gold particle
Ti	on the bulk titania, not neighboring gold

Table 2 gives the reaction mechanism for all processes occurring in the catalytic reactor. This mechanism includes all of the steps derived from our experimental observations, including catalyst deactivation and product readsorption. Reaction 1 is the propene reactive adsorption producing the bidentate propoxy species on titania near gold. Reaction 2 is the formation of a peroxide species on gold. Reaction 3 is the reaction of the peroxide species from the gold with the bidentate propoxy species to produce propene oxide. Reaction 4 is the deactivating reaction in which a bidentate propoxy species is further oxidized to strongly adsorbed carbonate/carboxylate species. Reactions 5 and 6 are reactive adsorption steps of propene oxide on titania near gold (5) and not near gold (6). As discussed earlier in this section, propene oxide desorption from the catalytic site is most likely the rate-determining step. In this reaction mechanism, this can imply that either reaction 2 or reaction 3 is the rate-determining step. Reaction 2 produces the peroxide species needed for desorption, and reaction 3 is the actual desorption step.

4. Reaction modeling

4.1. Reaction model

Using Athena Visual Workbench, the reaction kinetics associated with the steps in Table 2 were fit to one of the catalytic epoxidation experiments. In this model, only the concentration of propene oxide in the gas phase and on the different catalyst sites (in any adsorbed or decomposed form) are taken into account. The hydrogen, oxygen, and propene concentrations are assumed to be constant, which is an acceptable simplification

Table 3
Equations describing the kinetic reactor model

$$\frac{\partial C_{PO}}{\partial t} = -\frac{\phi_v}{A_r \cdot \varepsilon} \cdot \frac{\partial C_{PO}}{\partial x} + \varepsilon \cdot D \cdot \frac{\partial^2 C_{PO}}{\partial x^2} - k_a \cdot C_{PO} \cdot (1 - \theta_{PO,TiAu} - \theta_{Carb,TiAu}) \cdot N_{Ti} \cdot f_{TiAu} + k_d \cdot N_{Ti} \cdot f_{TiAu} \cdot \theta_{PO,TiAu} - k_a \cdot C_{PO} \cdot (1 - \theta_{PO,TiTi}) \cdot N_{Ti} \cdot (1 - f_{TiAu}) \quad (1)$$

$$\frac{\partial \theta_{PO,TiAu}}{\partial t} = k_r \cdot (1 - \theta_{PO,TiAu} - \theta_{Carb,TiAu}) + k_a \cdot C_{PO} \cdot (1 - \theta_{PO,TiAu} - \theta_{Carb,TiAu}) - k_d \cdot \theta_{PO,TiAu} - k_{deact} \cdot \theta_{PO,TiAu} \quad (2)$$

$$\frac{\partial \theta_{Carb,TiAu}}{\partial t} = k_{deac} \cdot \theta_{PO,TiAu} \quad (3)$$

$$\frac{\partial \theta_{PO,TiTi}}{\partial t} = k_a \cdot C_{PO} \cdot (1 - \theta_{PO,TiTi}) \quad (4)$$

Initial and boundary conditions

at $t = 0$: $C_{PO}, \theta_{PO,TiAu}, \theta_{PO,TiTi}, \theta_{Carb,TiAu} = 0$

at $x = 0$: $C_{PO} = 0$

at $x = L$: $\frac{\partial C_{PO}}{\partial x} = 0$

considering the very low conversions of these components. In addition, the availability of lattice oxygen is not taken into account. It is assumed that this is excessive compared with the number of titania sites on the catalyst surface, a reasonable assumption considering the low surface area of the catalyst. Furthermore, the lattice oxygen consumed in bidentate propoxy formation in reaction 2 is regenerated when propene oxide is produced in reaction 3. Table 3 gives the (differential) equations as they are solved and fitted to the experiments. The model focuses on propene oxide production and catalyst deactivation by fitting them to the measured propene oxide concentration in the catalytic experiments. Water concentrations are not fitted, even though water is produced in large quantities as a side product; thus the decomposition of the HOOH produced in reaction 2 is also not taken into account.

A plug flow reactor with axial dispersion was taken as a model for the reactor. This type of reactor was used because the experiments showed a "breakthrough curve"-type behavior of propene oxide through the catalyst bed as a result of the strong adsorption on titania. This type of behavior can be modeled only for a plug flow reactor. Axial dispersion was added to the model; this is very common in plug flow reactors and has the added advantage of smoothing out sharp steps in concentration as the propene oxide front moves through the reactor. (Sharp steps in concentration make transient differential equations more difficult to solve numerically.) The diffusivity was estimated using the equation developed by Fuller [21]. The bed porosity was estimated as 0.4, and the tortuosity was approximated as $1/\varepsilon$ ($= 2.5$).

The differential equations were all solved simultaneously to calculate the transient behavior of the reactor. The equations from Table 2 were all considered nonreversible, of a finite rate, and nonequilibrated. In the kinetic model 2, neighboring Ti sites on which propene or propene oxide can absorb were redefined as one catalytic site.

Equation (1) in Table 3 describes the change in the propene oxide concentration as a function of time at each axial position. The first term in the equation is the convective flow transport of propene oxide through the reactor, and the second term describes the diffusional transport in the axial direction. The third term represents the adsorption of propene oxide on titanium sites adjacent to a gold particle (reaction 5), and the fourth term describes the desorption of adsorbed propene oxide (the bidentate propoxy species) from the same sites (reaction 3). The final term in this equation represents the adsorption of propene oxide on titanium sites not adjacent to a gold particle (reaction 6).

Differential equation (2) calculates the time-dependent change of propene oxide on the titania sites adjacent to a gold particle and thereby contains most of the reactions from Table 2. The first term represents the formation of propene oxide (as bidentate propoxy) on these sites by the reactive adsorption of propene (reaction 1). This rate is dependent only on the number of vacant sites available for the reaction. The second and third terms in this equation represent the adsorption of propene oxide from the gas phase (reaction 5) and the desorption of the adsorbed propene oxide, respectively. In the mechanism shown in Table 2, this desorption step is assumed to be rate-determining and to occur only when aided by a reaction with a hydroperoxide species (OOH or H_2O_2) formed on the gold. Thus this third term is more a reaction than a simple desorption. It is assumed that this hydroperoxide species is a very reactive intermediate and reacts immediately with an adsorbed bidentate propoxy to produce propene oxide or decomposes directly to produce water. As a result, the concentration of the peroxide species is negligible, in agreement with the fact that this species has not yet been under reaction conditions during the epoxidation. It has been observed in the hydrogen peroxide production from hydrogen/oxygen over these catalysts [3], which also supports this assumption. Because the concentration of the hydroperoxide species is negligibly low, it is not included in the model. Formation of the peroxide species is rate-determining, and once this species is formed, it immediately reacts to produce (desorbed) propene oxide. In effect, the third term in Eq. (2) is a combination of those from reactions 2 and 3 from Table 2, and the rate constant and activation energy determined by the model for this step is actually a combination of those of two elementary steps. The last term in Eq. (2) represents the deactivating oxidative reaction of the adsorbed propene oxide to carbonate/carboxylate/formiate species (reaction 4).

Differential equation (3) represents formation of the carbonate/carboxylate/formiate species, effectively causing the catalyst to lose active sites (reaction 4). This deactivation rate is assumed to be first order in the concentration of adsorbed propene oxide on the catalytic sites. For a strongly adsorbing component (like propene oxide on this catalyst), this effectively results in a decay in catalytic activity that approaches an exponential decay. Differential equation (4) represents the adsorption of gas-phase propene oxide on titanium sites that are not adjacent to a gold particle (reaction 6). In concordance with the infrared

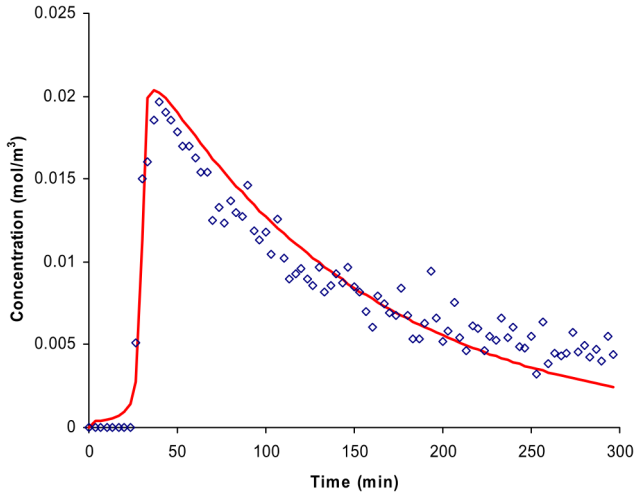

(a)

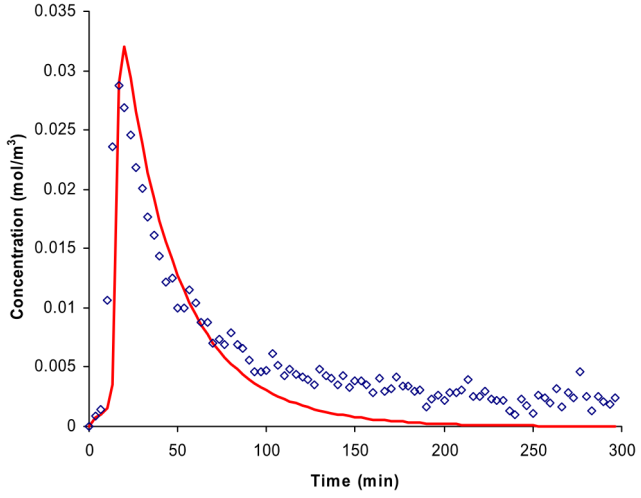

(b)

Fig. 7. Simulation of catalyst performance/deactivation for propene epoxidation over a 1 wt% Au/TiO_2 catalyst (GHSV = 9000 $m^3_{gas}/(m^3_{cat}\,h)$). Open symbols: model, closed: experiment. (a) 325 and (b) 345 K.

and gravimetrical experiments, the two species described in Eqs. (3) and (4) desorb from the catalyst surface at a negligible rate.

Fig. 7a compares the results of this calculation with those of a catalytic experiment. It can be seen that our proposed catalytic mechanism can describe the observed behavior relatively well at a reaction temperature of 325 K. However, Fig. 7b shows that at a somewhat higher temperature (345 K), this model cannot provide a good description of the experiment, because the residual activity of the deactivated catalyst is higher than predicted by the model.

4.2. Catalyst reactivation

The greater residual activity of the catalyst can be explained by a very slow desorption of the deactivating species from the catalyst, causing reactivation of the catalyst. Explaining this residual activity by, for example, competitive adsorption of water is not possible, because such an effect would still result in decreasing activity over time, but at the higher reaction temperatures, the activity remains constant after 2 h. The desorption of competitively adsorbing components would free up extra reaction sites, but would not stop the loss of sites due to the oxidation of the bidentate propoxy species. In the catalytic experiments we observed no other products than propene oxide at reaction temperatures <353 K, but the possibility exists that this desorption could occur with concentrations of the resulting side products below the detection limit (5×10^{-4} mol/m^3). Therefore, the site regeneration step was added to the model to determine whether this could explain the higher residual activity, and the concentrations of the side products formed in this manner were calculated.

Table 4
Extension to the kinetic reactor model in Table 2 to include catalyst reactivation

$$\frac{\partial \theta_{\mathrm{Carb,TiAu}}}{\partial t} = k_{\mathrm{deact}} \cdot \theta_{\mathrm{PO,TiAu}} - k_{\mathrm{react}} \cdot \theta_{\mathrm{Carb,TiAu}} \tag{3a}$$

$$\frac{\partial C_{\mathrm{SP}}}{\partial t} = -\frac{\phi_{\mathrm{v}}}{A_{\mathrm{r}} \cdot \varepsilon} \cdot \frac{\partial C_{\mathrm{SP}}}{\partial x} + \varepsilon \cdot D \cdot \frac{\partial^2 C_{\mathrm{SP}}}{\partial x^2} + k_{\mathrm{d}} \cdot N_{\mathrm{Ti}} \cdot f_{\mathrm{TiAu}} \cdot \theta_{\mathrm{Carb,TiAu}} \tag{6}$$

Initial and boundary conditions

at $t = 0$: $C_{\mathrm{SP}} = 0$

at $x = 0$: $C_{\mathrm{SP}} = 0$

at $x = L$: $\dfrac{\partial C_{\mathrm{SP}}}{\partial x} = 0$

Table 4 gives the extension to the reaction model to include reactivation of the catalyst when the carbonate and similar species formed on oxidation of the bidentate propoxy species desorb from the catalyst surface. Equation (3a) is the new equation calculating the amount of these species on the catalyst surface [replacing Eq. (3)]. Equation (6) calculates the concentration of side products in the gas phase that must be formed as the catalyst is reactivated.

The model including catalyst reactivation can describe the measured catalytic performance well. To determine the kinetic parameters and evaluate the model's performance at different experimental conditions, the model was fitted to one mixed dataset of experimental observations. This dataset comprised 15 experiments, each with about 100 data points in time measured at 6 different reaction temperatures, 4 different gas feed rates, and 2 different catalyst masses. Thus the total number of experimental observations was 1500. Seven "normal" parameters were fitted to the experiments: k_{a}, the rate constant for propene oxide adsorption; N_{Ti}, the number of (adsorption) sites on the titania; f_{TiAu}, the fraction of the titania sites neighboring a gold particle; k_{d}, the desorption rate of propene oxide;[2] k_{r}, the reaction rate constant producing bidentate porpoxy species on the catalyst out of propene; k_{deact}, the rate constant for the deactivation of the catalyst (i.e., the conversion of the bidentate propoxy species to carbonate species); and k_{react}, the rate constant for

[2] Note: this is not a simple desorption, but rater a reaction step. PO adsorbed on titania as a bidentate propoxy is observed not to desorb. Only in the presence of hydrogen and oxygen (in our model assumed to produce a peroxide species) it desorbs.

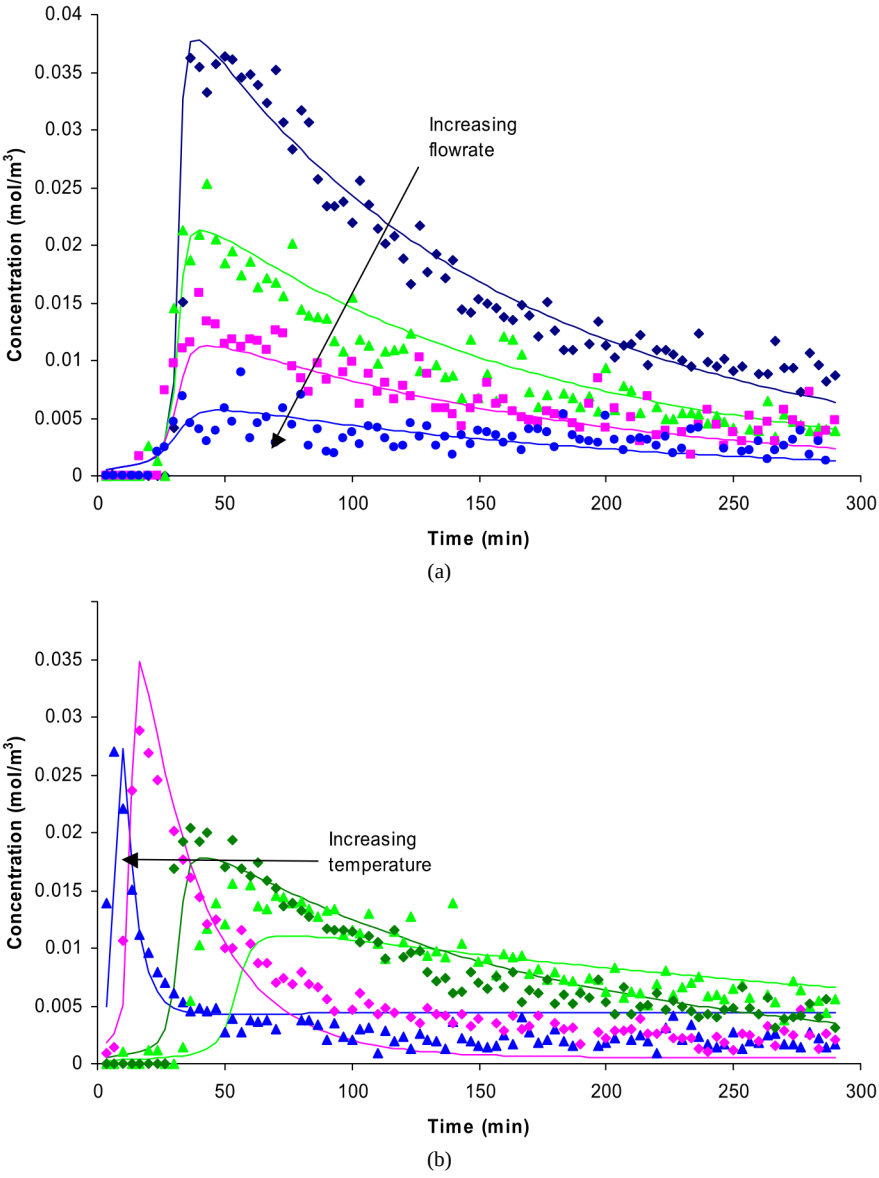

Fig. 8. Comparison between measured and modeled behavior of 1 wt% Au/TiO_2 catalyst for the epoxidation of propene. (a) Activity at different flow rates (325 K, GHSV 4500–36 000 $m^3_{gas}/(m^3_{cat}\,h)$). (b) Activity at different reaction temperatures (GHSV 9000 $m^3_{gas}/(m^3_{cat}\,h)$, $T = 315$–366 K).

the reactivation of the catalyst by desorption of the carbonate species. In addition, four activation energies were fitted to the experiments to account for the rate constants being a function of temperature. For k_d, k_r, k_{deact}, and k_{react}, activation energies were calculated according to an Arrhenius equation. N_{Ti} and f_{TiAu} are parameters that describe the nature of the catalyst and thus are temperature-independent. The parameter k_a was also assumed to be temperature-independent. The rate of adsorption is a function of the number of collisions of the adsorbing molecule with free adsorption sites. The collision frequency increases proportionally to the square root of the temperature, and the change in this quantity over the temperature range of the modeled experiments (315–365 K) is small. As a simplification and a means of reducing the total number of parameters, this dependency was neglected. Using the same arguments, the same adsorption rate constant was used for sites near and not near gold particles.

Fig. 8 shows the results of the kinetic modeling for a selection of flow rates and temperatures. The model describes the observed catalyst performance well. There are differences between the measurements and the model for individual experiments, but considering that the model was fitted to a large dataset of separate experiments and with only one set of parameters that apply for all conditions, the fits are remarkably good. Differences in the reaction conditions caused by the fact that the reactor had a different catalyst loading for each separate experimental run are not accounted for. The model cannot adjust for such changes in the experiments as channeling through the catalyst bed or using different locations for temperature measurement; the parameter values represent the average situation for all experiments. The only significant difference is that the model slightly overpredicts the propene oxide production at the highest reaction temperatures. This difference can be explained by the decrease in reaction selectivity with increasing

Table 5
Summary of parameters obtained from fitting the kinetic model to the experimental data set (rate constants at 325 K)

Parameter	Units	Value	95% confidence region	
			Lower	Upper
k_r	min^{-1}	1.18	0	2.4
k_a	$m^3/(mol\,min)$	70.9	25	117
k_d	min^{-1}	2.63	0	6.2
k_{deact}	min^{-1}	0.0202	0.004	0.036
k_{react}	min^{-1}	1.08×10^{-5}	8.5×10^{-6}	1.3×10^{-5}
N_{Ti}	mol/m^3	282	220	340
f_{TiAu}	–	0.043	0.005	0.081
$E_{a,r}$	kJ/mol	47.5	36	58
$E_{a,d}$	kJ/mol	46.8	24	69
$E_{a,deact}$	kJ/mol	144	133	154
$E_{a,react}$	kJ/mol	81.9	60	104

reaction temperature. The side reactions that lead to this decreased selectivity are not included in the model.

Table 5 gives the parameters obtained by fitting the model to the experiments. These parameter values are all physically feasible. The adsorption capacity of 282 mol/m^3 corresponds to an adsorption capacity of 1.4 wt% (bulk density of 1200 kg/m^3), which corresponds very well to the gravimetrically determined adsorption capacity given in Table 1. The fraction of 4/100 sites neighboring gold is also a reasonable value considering the coverage with gold particles of the catalyst shown in Fig. 1. The fact that the activation energy for catalyst deactivation is higher than the other activation energies is in agreement with the observation that the yield for the propene oxide production decreases with increasing reaction temperature. The two activation energies involved in the production of propene oxide, $E_{a,r}$ and $E_{a,d}$, both have a value of about 47 kJ/mol. This is higher than the observed activation energy for propene oxide production of about 30 kJ/mol that can be calculated from Fig. 6a. However, it should be noted that this value of 30 kJ/mol is a value for the observed amount of propene oxide in the gas phase. Therefore, this value must be lower than the true activation energy for propene oxide production, because the deactivating side reaction (bidentate propoxy oxidation) increases more rapidly with an increasing temperature, thereby decreasing the apparent activation energy. Qualitative examination of the surface occupancies on the catalyst reveals that increasing surface coverage with carbonate species agrees with increasing catalyst deactivation. The remaining portions of the available surface sites are about half covered with bidentate propoxy species, indicating that indeed reaction 2 or 3 is the rate determining step. Because the model does not calculate peroxide concentrations, we cannot determine which of these two steps is actually the rate-determining step. We also see that as propene oxide begins to appear in the gas phase in the model, the titania sites nonadjacent to gold are almost completely covered with adsorbed propene oxide as bidentate propoxy species.

In the model, catalyst reactivation is assumed to occur through desorption of the deactivating species. In this case the products desorbing from the catalyst are carbon dioxide, ethanal, and methanol. The first two of these are the most important side products observed at lower temperatures. To check whether their quantity is in agreement with the experimental observation that the selectivity at low temperatures is close to 100%, we used Eq. (6) to calculate the concentration of these species in the gas phase. These calculations showed that at a reaction temperature of 325 K, the concentration of these species was at most 10^{-6} mol/m^3. The highest value at 366 K was 2×10^{-4} mol/m^3. These concentrations are much lower than the propene oxide concentrations (typically 0.01 mol/m^3) and are in agreement with the observed high selectivity.

Although these calculations confirm the high selectivity observed for this reaction, the actual selectivity in this study and reported in literature is not as close to 100% as is generally assumed. These high selectivities are based on all observed products; usually a better way to calculate selectivity is to do so based on the amounts of product formed and reactant converted. However, for this reaction, the very low propene conversions (<1%) make calculations based on reactant conversion unreliable, because the reactant conversion is calculated from a small change in a large value and thus has an associated high-percentage error. Our thermogravimetric experiments and modeling work demonstrated that the catalyst retains a lot of propene oxide in the form of a bidentate propoxy species during the reaction. Comparing the quantity estimated from Fig. 5 (0.7 wt% adsorbed = 0.04 mmol) with the quantity of propene oxide produced during a 5-h experimental run (typically 0.1–0.3 mmol) reveals that the actual selectivity of these so-called "highly selective" catalysts is only 80%.

5. Discussion

Our proposed kinetic model gives a good description of the catalytic data; however, improvement is still possible. For example, competitive adsorption of water, as well as the reactions leading to the side products, could be added. Writing down the model equations for these additions is relatively simple; however, both the number of equations to solve and the number of experimental observations to fit will increase significantly, making this computationally very challenging. We hope that this will be possible in the near future.

In our model we show that on propene adsorption on the catalyst, a bidentate propoxy species is formed in which the oxygen originates from the titania lattice. This is based on our observations [9,20] in adsorption experiments in an infrared cell in the absence of oxygen that a bidentate propoxy species can be formed out of propene. For the kinetic modeling work that we present here, it is not an absolute necessity to stick to this mechanism using lattice oxygen. The same equations as presented in Tables 3 and 4 would still be valid if propene would simply adsorb on titania and then undergo oxidation by an oxidizing species like a peroxide formed on gold to produce propene oxide. The propene oxide could readsorb and be oxidized further toward a strongly adsorbed carbonate species, causing deactivation. This would be close to the more general assumption in the literature for the reaction mechanism as discussed in the Introduction. Such a model would also be able to describe our measurements. The rate constants and activation energies

would be the same, but would correspond to different mechanistic steps.

As a final remark, we would like to make clear that our kinetic modeling work provides no conclusive proof that the reaction mechanism that we propose is correct. It does prove, however, that the reaction mechanism is capable of describing the observed catalytic behavior and thus that the mechanism is consistent with the experimental data.

6. Conclusions

A kinetic model is presented that can describe the performance of gold–titania catalysts for propene epoxidation up to a reaction temperature of 365 K. The kinetic model can describe experiments at a range of temperatures and space velocities with one single set of parameters, the values of which are all physically feasible.

Propene oxide is produced by reactive adsorption of propene on titania sites near the gold nanoparticles, producing a bidentate propoxy species. The desorption of this species occurs only when hydrogen and oxygen are co-fed, at which time propene oxide is produced in the gas phase. This step is rate-determining. Catalyst deactivation occurs through further oxidation of the bidentate propoxy reaction intermediate to carboxylates/formiates.

Acknowledgments

STW/NWO and NWO/CW are kindly acknowledged for the VIDI funding (to T.A.N.) and the VICI funding (to B.M.W.). The authors thank C. van de Spek and A. Broersma for providing TEM and thermogravimetric measurements.

Appendix A. Nomenclature

A.1. Symbols

A_r	reactor cross sectional area, m^2
C	gas phase concentration, mol/m^3
D	(gas phase) diffusivity, m^2/s
f_{TiAu}	fraction of Ti sites neighboring gold, –
k	rate constant, $1/s$
L	reactor/catalyst bed length, m
N_{Ti}	Ti site concentration, mol/m^3
t	time, s
x	(axial) position in reactor, m
ε	catalyst bed porosity, –
ϕ_v	volumetric gas flow rate, m^3/s
θ	surface occupancy, –

A.2. Subscripts

PO	propene oxide
SP	side product
TiAu	titanium neighboring gold
TiTi	titanium not neighboring gold
a	adsorption
d	desorption
r	reaction
deact	deactivation by oxidation of bidentate propoxy
react	catalyst reactivation by desorption of deactivating species

References

[1] T. Hayashi, K. Tanaka, M. Haruta, J. Catal. 178 (1998) 566.
[2] T.A. Nijhuis, B.J. Huizinga, M. Makkee, J.A. Moulijn, Ind. Eng. Chem. Res. 38 (1999) 884.
[3] C. Sivadinarayana, T.V. Choudhary, L.L. Daemen, J. Eckert, D.W. Goodman, J. Am. Chem. Soc. 126 (2004) 38.
[4] M.G. Clerici, G. Bellussi, U. Romano, J. Catal. 129 (1991) 159.
[5] D.G. Barton, S.G. Podkolzin, J. Phys. Chem. B 109 (2005) 2262.
[6] D.H. Wells, W.N. Delgass, K.T. Thomson, J. Catal. 225 (2004) 69.
[7] P.P. Olivera, E.M. Patrito, H. Sellers, Surf. Sci. 313 (1994) 25.
[8] T. Ishihara, Y. Ohura, S. Yoshida, Y. Hata, H. Nishiguchi, Y. Takita, Appl. Catal. A: Gen. 291 (2005) 215.
[9] T.A. Nijhuis, T. Visser, B.M. Weckhuysen, Angew. Chem. Int. Ed. 44 (2005) 1115.
[10] J.M. Fisher, Gold Bull. 36 (2003) 155.
[11] A. Zwijnenburg, M. Makkee, J.A. Moulijn, Appl. Catal. A: Gen. 270 (2004) 49.
[12] T.A. Nijhuis, B.M. Weckhuysen, Chem. Commun. (2005), in press.
[13] E.E. Stangland, K.B. Stavens, R.P. Andres, W.N. Delgass, J. Catal. 191 (2000) 332.
[14] G. Mul, A. Zwijnenburg, B. van der Linden, M. Makkee, J.A. Moulijn, J. Catal. 201 (2001) 128.
[15] R.G. Bowman, H.W. Clark, A. Kuperman, G.E. Hartwell, G.R. Meima, US Patent 6670491 (2003), to DOW.
[16] G.R. Meima, H.W. Clark, R.G. Bowman, A. Kuperman, G.E. Hartwell, US Patent 6646142 (2003), to DOW.
[17] P. Landon, P.J. Collier, A.J. Papworth, C.J. Kiely, G.J. Hutchings, Chem. Commun. (2002) 2058.
[18] D. Eder, R. Kramer, Phys. Chem. Chem. Phys. 5 (2003) 1314.
[19] W.S. Epling, C.H.F. Peden, M.A. Henderson, U. Diebold, Surf. Sci. 413 (1998) 333.
[20] T.A. Nijhuis, T. Visser, B.M. Weckhuysen, J. Phys. Chem. B (2005), in press; DOI: 10.1021/jp053173p.
[21] B.E. Poling, J.M. Prausnitz, J. O'Connel, The Properties of Gases and Liquids, fifth ed., McGraw–Hill, New York, 2001.